utilization in the temporal cortex of affectively ill patients: positron emission tomography. *Biol Psychiatry* 1987;22:545–553.
9. Kanaya T, Yonekawa M. Regional cerebral blood flow in depression. *Jpn J Psych Neurol* 1990;44:571–576.
10. Austin MP, Dougall N, Ross M, et al. Single-photon emission tomography with ^{99m}Tc-exametazime in major depression and the pattern of brain activity underlying the psychotic/neurotic continuum. *J Affect Disord* 1992;26:31–43.
11. Mayberg HS, Jeffrey PJ, Wagner HN, Simpson SG. Regional cerebral blood flow in patients with refractory unipolar depression measured with ^{99m}Tc-HMPAO/SPECT [Abstract]. *J Nucl Med* 1991;32:951.
12. Kazim MY, Ozlem K, Belkis E, Erhan V, Cengiz G, Coskun FB. Assessment of changes in regional cerebral blood flow in patients with major depression using ^{99m}Tc-HMPAO single-photon emission tomography method. *Eur J Nucl Med* 1992; 19:1038–1043.
13. Delvenne V, Delecluse F, Hubain PP, Schoutens A, DeMaertelaer V, Mendlewicz J. Regional cerebral blood flow in patients with affective disorders. *Br J Psychiatry* 1990;157:359–365.
14. Schlegel S, Aldenhoff JB, Eissner D, Lindner P, Nickel O. Regional cerebral blood flow in depression: associations with psychopathology. *J Affective Disord* 1989;17: 211–218.
15. Sackeim HA, Prohovnik I, Moeller JR, et al. Regional cerebral blood flow in mood disorders. *Arch Gen Psychiatry* 1990;47:60–70.
16. Mathew RJ, Meyer JS, Francis DJ, Semchuk KM, Mortel K, Claghorn JL. Cerebral blood flow in depression. *Am J Psychiatry* 1980;137:1449–1450.
17. Silfverskiold P, Risberg J. Regional cerebral blood flow in depression and mania. *Arch Gen Psychiatry* 1989;46:253–259.
18. Goldstein PC, Brown GG, Welch KMA, Marcus A, Ewing JR, Rosenbaum G. Age-related decline of rCBF in schizophrenia and major affective disorder. *J Cereb Blood Flow Metab* 1985;5:203–204.
19. Gur RE, Skolnick BE, Gur RC, et al. Brain function in psychiatric disorders. II: regional cerebral blood flow in medicated unipolar depressives. *Arch Gen Psychiatry* 1984;41:695–699.
20. Volk S, Kaendler SH, Weber R, et al. Evaluation of the effects of total sleep deprivation on cerebral blood flow using single-photon emission computed tomography. *Acta Psychiatr Scand* 1992;86:478–483.
21. Ebert D, Feistel H, Barocka A. Effect of sleep deprivation on the limbic system and frontal lobes in affective disorders: a study with ^{99m}Tc-HMPAO SPECT. *Psychiatry Res Neuroimaging* 1991;40:247–251.
22. Wu JC, Gillin JC, Buchsbaum MS, Hershey T, Johnson JC, Bunney WE. Effect of sleep deprivation on brain metabolism of depressed patients. *Am J Psychiatry* 1992;149:538–543.
23. Silfverskiold P, Gustafson L, Risberg J, Rosen I. Acute and late effects of electroconvulsive therapy: clinical outcome of regional cerebral blood flow and electroencephalogram. *Ann NY Acad Sci* 1986;462:236–248.
24. Prohovnik I, Sackeim HA, Decina P, Malitz S. Acute reductions of regional cerebral blood flow following electroconvulsive therapy. Interactions with modality and time. *Ann NY Acad Sci* 1986;462:249–262.
25. Rosenberg R, Vostrup S, Andersen A, Bolwig T. Effect of ECT on cerebral blood flow in melancholia assessed with SPECT. *Convulsive Ther* 1988;4:62–73.
26. Scott AIF, Dougall N, Ross M, et al. Short-term effects of electroconvulsive treatment on the uptake of ^{99m}Tc-exametazime into brain in major depression with single photon tomography. *J Affective Disord* 1994;30:37–44.
27. Volkow ND, Bellar S, Mullani N, Jould L, Dewey S. Effects of electroconvulsive therapy on brain glucose metabolism: a preliminary study. *Convulsive Ther* 1988;4: 199–205.
28. Guze BH, Baxter LR Jr, Schwartz JM, Szuba MP, Liston EH. Electroconvulsive therapy and brain glucose metabolism. *Convulsive Ther* 1991;7:15–19.
29. Nobler MS, Sackeim HA, Prohovnik I, et al. Regional cerebral blood flow in mood disorders. III. treatment and clinical response. *Arch Gen Psychiatry* 1994;51:884–897.
30. American Psychiatric Association. *Diagnostic and statistical manual of mental disorders*, 3rd ed. rev. Washington, DC: American Psychiatric Association; 1987.
31. Hamilton M. A rating scale for depression. *J Neurol Neurosurg Psychiatry* 1960;23: 56–62.
32. Sackeim HA, Decina P, Prohovnik I, Malitz S. Seizure threshold in ECT. *Arch Gen Psychiatry* 1987;44:355–360.
33. Talairach J, Zilkha G, Tournoux P, et al. *Atlas d'anatomie stereotactique du telencephale.* Masson; Paris: 1988.
34. Rubin RT, Villanueva-Meyer J, Ananth J, Trajmar PG, Mena I. Regional xenon-133 cerebral blood flow and cerebral technetium-99m-HMPAO uptake in unmedicated patients with obsessive-compulsive disorder and matched normal control subjects. *Arch Gen Psychiatry* 1992;49:695–702.
35. Baxter LR. Brain imaging as a tool in establishing a theory of brain pathology in obsessive-compulsive disorder. *J Clin Psych* 1990;51(suppl):22–25.
36. Kung HF. New technetium-99m-labeled brain perfusion imaging agents. *Semin Nucl Med* 1990;2:150–158.
37. Mayberg HS, Lewis PJ, Regenold W, Wagner HN Jr. Paralimbic hypoperfusion in unipolar depression. *J Nucl Med* 1994;3:929–934.
38. Robinson RG, Kubos KL, Starr LB, et al. Mood disorders in stroke patients: importance of location of lesion. *Brain* 1984;107:81–93.
39. Starkstein SE, Robinson RG, Price TR. Comparison of cortical and subcortical lesions in the production of post-stroke mood disorders. *Brain* 1987;110:1045–1059.
40. Grafman J, Vance SC, Weingartner H, et al. The effects of lateralized frontal lesions on mood regulation. *Brain* 1986;109:1127–1148.
41. Ross ED, Rush AJ. Diagnosis and neuroanatomical correlates of depression in brain-damaged patients. *Arch Gen Psychiatry* 1981;39:1344–1354.
42. Altshuler LL, Devinsky O, Post RM, Theodore W. Depression, anxiety and temporal lobe epilepsy: laterality of focus and symptoms. *Arch Neurol* 1990;47:284–288.

Measurement of Regional Cerebral Plasma Pool and Hematocrit with Copper-62-Labeled HSA-DTS

Hidehiko Okazawa, Yoshiharu Yonekura, Yasuhisa Fujibayashi, Hiroshi Yamauchi, Koichi Ishizu, Sadahiko Nishizawa, Yasuhiro Magata, Nagara Tamaki, Hidenao Fukuyama, Akira Yokoyama and Junji Konishi
Faculties of Medicine and Pharmaceutical Sciences, Kyoto University, Kyoto; and Biomedical Imaging Research Center, Fukui Medical School, Fukui, Japan

We developed copper-62-labeled human serum albumin-dithiosemicarbazone (^{62}Cu-HSA-DTS) as a blood-pool imaging agent for PET. To evaluate ^{62}Cu-HSA-DTS for plasma-pool imaging and to measure the regional cerebral hematocrit, 12 normal volunteers and 7 patients with cerebrovascular disease underwent PET studies with ^{62}Cu-HSA-DTS and ^{15}O-labeled carbon monoxide ($C^{15}O$). **Methods:** The normal subjects were studied with both $C^{15}O$ and ^{62}Cu-HSA-DTS. All patients were examined by ^{15}O-gas studies to measure cerebral perfusion and oxygen metabolism, followed by measurement of plasma volume with ^{62}Cu-HSA-DTS for analysis of regional cerebral hematocrit. Regional cerebral hematocrit was calculated from regional cerebral red cell volume (rCRCV) measured by $C^{15}O$ and regional plasma volume (rCPV) measured by ^{62}Cu-HSA-DTS in each subject, and the regional cerebral/large-vessel hematocrit ratio was obtained for both cerebral hemispheres in each subject. **Results:** Mean regional cerebral hematocrit and mean cerebral/large-vessel hematocrit ratio in the 12 normal volunteers were 38.3 ± 3.45% and 0.88 ± 0.06, respectively. In the seven patients with cerebrovascular disease, regional cerebral hematocrit was significantly lower on the hypoperfused side than the normal hemisphere. The images of rCPV and rCRCV from these patients demonstrated a greater increase in rCPV than rCRCV in the hypoperfused area. **Conclusion:** These results suggest that ^{62}Cu-HSA-DTS can be used for measurement of plasma volume and that regional cerebral hematocrit may provide valuable information regarding the microcirculation in the brain.

Key Words: PET; copper-62-labeled human serum albumin-dithiosemicarbazone; plasma volume; regional hematocrit

J Nucl Med 1996; 37:1080–1085

Received May 22, 1995; revision accepted Oct. 20, 1995.

For correspondence or reprints contact: Hidehiko Okazawa, MD, Montreal Neurological Institute, Cyclotron Unit, McGill University, 3801 University St., Montreal, Quebec, Canada H3A 2B4.

The $^{62}Zn/^{62}Cu$ positron generator has been proposed as a possible source of generator-produced radiopharmaceuticals for positron emission tomography (PET) studies without use of an in-house cyclotron (*1*), and copper (II) pyruvaldehyde bis(N^4-methylthiosemicarbazone) labeled with ^{62}Cu (^{62}Cu-PTSM) has been applied as a perfusion tracer (*2–6*). For the plasma-pool imaging agent, ^{62}Cu-labeled human serum albumin-dithiosemicarbazone (^{62}Cu-HSA-DTS) (*7*) and benzyl-1,4,8,11-tetraazacyclotetradecan-N,N′,N″,N‴-tetraacetic acid-albumin (^{62}Cu-benzyl-TETA-HSA) (*8*) were developed and investigated. Measurement of plasma volume and red cell volume enables estimation of the regional cerebral hematocrit (Hct), and several such investigations in the human brain have been reported (*9–14*). In tomographic measurement of cerebral Hct in human brain, the regional cerebral/large-vessel Hct ratio (Hct ratio: *r*) was reported to be 0.69 in a PET study by Lammertsma et al. (*11*), 0.76 in a SPECT study by Sakai et al. (*12*) and 0.87 in a SPECT study of normal subjects by Loutfi et al. (*14*).

In the present study, ^{62}Cu-HSA-DTS was used as a cerebral plasma volume imaging agent, and regional cerebral Hct was measured with this agent and ^{15}O-labeled carbon monoxide ($C^{15}O$) in normal volunteers and patients with cerebrovascular disease. In the normal subjects, we sought to confirm the normal cerebral Hct ratio using ^{62}Cu-HSA-DTS and to evaluate the feasibility of measurement of regional cerebral Hct in a clinical study. In the patients, the chronic stage of cerebrovascular disease was investigated and compared with the acute stage of stroke reported previously (*14,15*).

MATERIALS AND METHODS

Preparation of Copper-62-HSA-DTS

A $^{62}Zn/^{62}Cu$ generator was prepared with $^{62}ZnCl_2$ aqueous solution (1.1 GBq, pH 5.0), and HSA-DTS was synthesized by the method reported previously (*7,16*). The ^{62}Cu labeling of HSA-DTS was performed by simple mixing of 4 ml of an HSA-DTS solution (5 mg/ml in saline buffer [pH 6.0]) and 4 ml of the ^{62}Cu generator eluate. The ^{62}Cu-HSA-DTS was easily obtained by a ligand-exchange reaction (*7*).

Subjects

The study included 12 normal male volunteers (24–46 yr old) and 7 patients with cerebrovascular disease confirmed by angiography (Table 1). All 12 normal subjects were studied with both ^{15}O-labeled carbon monoxide ($C^{15}O$) and ^{62}Cu-HSA-DTS by blood sampling from the cubital vein. Six of the 12 normal subjects also underwent a ^{15}O-labeled water study to obtain cerebral blood flow (CBF) images. All seven patients underwent ^{15}O-gas studies to measure cerebral perfusion and oxygen metabolism with arterial blood sampling and a ^{62}Cu-HSA-DTS study to measure regional plasma volume for analysis of regional Hct. The PET study was carried out under the guidance of the Ethical Committee of the Faculty of Medicine of Kyoto University, and written informed consent was obtained from all subjects before the study.

PET Images

PET images were obtained from a scanner (*6,17*) that permits simultaneous acquisition of 15 transverse slices with a center-to-center distance of 7 mm. All scans were performed at a resolution of 9-mm FWHM in the transaxial direction and 6.5 mm in the axial direction. The field of view and pixel size of the reconstructed images were 256 and 2 mm, respectively.

The subject's head was immobilized with a head-holder. The head was positioned with light beams to obtain transaxial slices parallel to the orbitomeatal (OM) line. In the normal volunteers, a small cannula was placed in the cubital vein contralateral to the administration side of the tracer. In the patients, a small cannula was placed in the brachial artery. Before all emission measurements, tomographic transmission data were obtained using a standard plate source of $^{68}Ge/^{68}Ga$ for attenuation correction. The tissue activity concentration in the PET images was cross-calibrated against a scintillation counter using a cylindrical phantom filled with ^{18}F solution.

For the ^{15}O-gas study in the patients, ^{15}O-labeled carbon dioxide ($C^{15}O_2$) and molecular oxygen ($^{15}O_2$) were inhaled continuously at 300 and 500 MBq/min, respectively, and the scan time was 5 min. The $C^{15}O$ was inhaled as a single dose of 1200 MBq, and the PET scan was started 30 sec after the arrival of the peak count of the brain tissue and continued for 3 min. Arterial blood was sampled three times during each scan of the $C^{15}O_2$ and $^{15}O_2$ studies and twice for the $C^{15}O$ study. For the $C^{15}O$ study in the normal subjects, venous blood was sampled as in the study of the patients. The blood samples thus obtained were immediately measured with the scintillation counter to determine arterial radioactivity. The CBF, oxygen extraction fraction (OEF) and cerebral metabolic rate of oxygen ($CMRO_2$) were obtained by the steady-state method (*18*). The cerebral blood volume (CBV) was calculated from the $C^{15}O$ scan data and was incorporated into the correction of the vascular space for $CMRO_2$ and OEF (*19*). In the calculation of CBV, a conventional Hct ratio of 0.85 was used.

To obtain plasma volume images, 296–740 MBq (8–20 mCi) of ^{62}Cu-HSA-DTS was injected intravenously over 15 sec in a total volume of 8 ml. PET data acquisition was started 3 min after administration of ^{62}Cu-HSA-DTS and continued for 8 min. Blood samples were obtained at 1, 5 and 7 min after injection of ^{62}Cu-HSA-DTS, and both whole-blood and plasma radioactivity were counted. In six normal subjects, a CBF image with relative values was obtained by a noninvasive method with ^{15}O-water (*20*) 15 min before the ^{62}Cu-HSA-DTS study for reference in selecting the regions of interest (ROIs).

TABLE 1
Clinical Characteristics of Seven Patients with Cerebrovascular Disease

Patient no.	Age	Sex	Disease	Time after onset	MRI findings
1	74	M	RICA occlusion	2.2 yr	Several lacunar infarcts, including right basal ganglia
2	63	M	RICA occlusion	2 mo	Subcortical infarction in right frontal lobe
3	62	F	RICA occlusion	3.4 yr	Some lacunar infarcts and mild brain atrophy
4	61	M	LICA occlusion	2.5 yr	Some lacunar infarcts in left cerebral hemisphere
5*	61	F	RICA occlusion	>1 yr	Occlusion of RICA
6	49	F	RMCA occlusion	1 mo	Subcortical infarction in right hemisphere
7	69	M	LICA occlusion	5.3 yr	Left parietal infarction, including cortex

*Right internal carotid artery (RICA) occlusion was found accidentally on MRI more than 1 yr before PET study.
LICA = left internal carotid artery; RMCA = right middle cerebral artery.

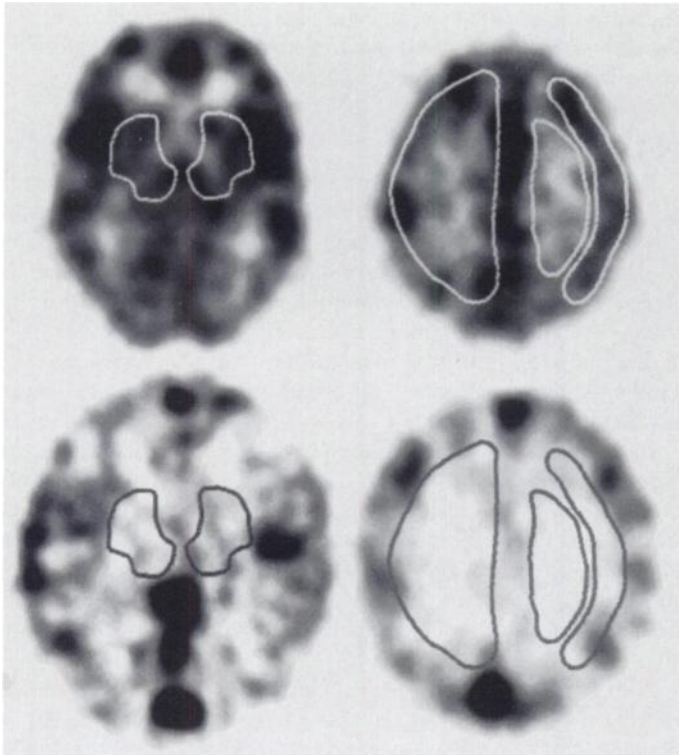

FIGURE 1. Regions of interest for bilateral basal ganglia (left), right hemisphere and left gray and white matter (right) are demonstrated for both CBF (top) and ^{62}Cu-HSA-DTS (bottom) images. Regions of interest for the right hemisphere and gray and white matter were placed bilaterally at the level of +70 mm above the OM line.

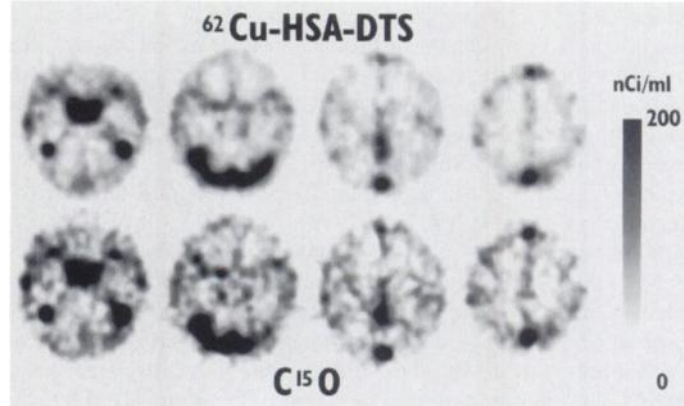

FIGURE 2. Cerebral tissue activity images from a normal volunteer obtained with the data 3–11 min after administration of ^{62}Cu-HSA-DTS (top). Excellent ^{62}Cu-HSA-DTS images were obtained compared with $C^{15}O$ images from the same subject (bottom).

Data Analysis

Regional cerebral red cell volume (rCRCV) and plasma volume (rCPV) were calculated according to the following equations using the PET images of the $C^{15}O$ and ^{62}Cu-HSA-DTS studies:

$$\text{rCRCV} = \frac{C_{CO}}{A_{CO}/h} \quad \text{(ml/g)}, \qquad \text{Eq. 1}$$

$$\text{rCPV} = \frac{C_{HSA}}{P_{HSA}} \quad \text{(ml/g)}, \qquad \text{Eq. 2}$$

where C_{CO} and C_{HSA} are the cerebral tissue radioactivity of $C^{15}O$ and ^{62}Cu-HSA-DTS, respectively; A_{CO} is the whole-blood radioactivity of $C^{15}O$; P_{HSA} is the plasma count of ^{62}Cu-HSA-DTS; and h is the hematocrit of the sampled blood, respectively. The regional cerebral Hct (rHct) was calculated from rCRCV and rCPV for each subject as follows:

$$\text{rHct} = \frac{\text{rCRCV}}{\text{rCRCV} + \text{rCPV}} \times 100(\%), \qquad \text{Eq. 3}$$

and the regional cerebral/large-vessel Hct ratio (r) was obtained for each cerebral hemisphere individually:

$$r = \frac{\text{rHct}}{h}. \qquad \text{Eq. 4}$$

In six normal subjects with CBF images and seven patients with cerebrovascular disease, ROIs were placed on the bilateral hemispheres at the level of the centrum semiovale (about +70 mm above the OM line), including large areas of the cerebral cortex, subcortex and white matter by referring to the CBF images, and the same ROIs were transferred to all images for each subject (Fig. 1). Regions of interest were also placed on the bilateral gray and white matter at the level of the centrum semiovale (+70 mm above the OM line) and the bilateral basal ganglia at the level of the thalamus (about +40 mm above the OM line) (Fig. 1) in six normal volunteers with CBF images. Large vessels were excluded by confirming the ROIs placed on the $C^{15}O$ or ^{62}Cu-HSA-DTS images. The levels of ROIs were selected to exclude the effect of large vessels in the cortical surface or basal areas or nonactivity in the ventricles. The ROIs were placed irrespective of the presence of infarction in the patients. The rCRCV, rCPV, rHct and Hct ratio were calculated for these areas. In the other six normal subjects without CBF images, large ROIs were placed on the bilateral hemispheres at the same level from the OM line as described previously. The Hct ratio *(r)* was also calculated from the equation proposed by Lammertsma et al. (*11*), which uses only the count of the whole-blood radioactivity of each tracer, so that we could compare the Hct ratios obtained by the method of Lammertsma et al. with those of our method.

The signal-to-noise ratios (S/N ratio; mean activity/s.d.) measured with the same ROIs in each hemisphere determined previously were obtained and compared between the $C^{15}O$ images and ^{62}Cu-HSA-DTS images of the 12 normal subjects. The S/N ratio in each image and the differences in the regional variables (rCRCV, rCPV, rHct and Hct ratio) in each area for six normal subjects were compared using analysis of variance (ANOVA) with a post hoc Scheffé's F-test. In the patients with cerebrovascular diseases, comparison between both hemispheres was performed with the paired t-test for each variable. A probability value of less than 0.05 was considered to indicate a significant difference.

RESULTS

Normal Volunteers

The generator system in the present study was able to provide ^{62}Cu eluate at an interval of every 40–60 min in the activity of 296–740 MBq (8–20 mCi). Figure 2 shows the cerebral tissue activity image from a normal volunteer obtained from data acquired 3–11 min after administration of ^{62}Cu-HSA-DTS and the corresponding cerebral tissue activity image obtained from the $C^{15}O$ study. The longer scan time in the ^{62}Cu-HSA-DTS study provided a less noisy image than with the $C^{15}O$ image. The average S/N ratio obtained with large ROIs on 24 hemispheres was 1.88 ± 0.32 for the $C^{15}O$ images and 2.33 ± 0.47 for the ^{62}Cu-HSA-DTS images. The S/N ratios obtained from ^{62}Cu-HSA-DTS images were significantly better than those of $C^{15}O$ images ($p < 0.0005$). From analysis of the venous blood samples, more than 97% of the radioactivity existed in the plasma pool during the PET study.

Table 2 summarizes the mean values of the rCRCV, rCPV

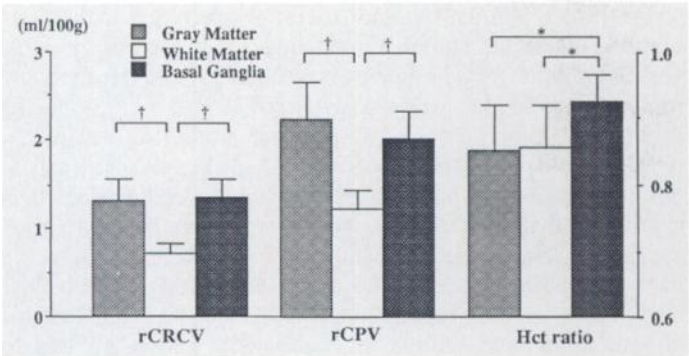

FIGURE 3. Mean values of rCRCV, rCPV and Hct ratio in the gray matter, white matter and basal ganglia in six normal subjects (mean ± s.d.). The rCRCV and rCPV values were significantly lower in the white matter than in the cortex or basal ganglia. The Hct ratio was significantly greater in the basal ganglia than in the gray or white matter. *$p < 0.05$, †$p < 0.0001$ by analysis of variance.

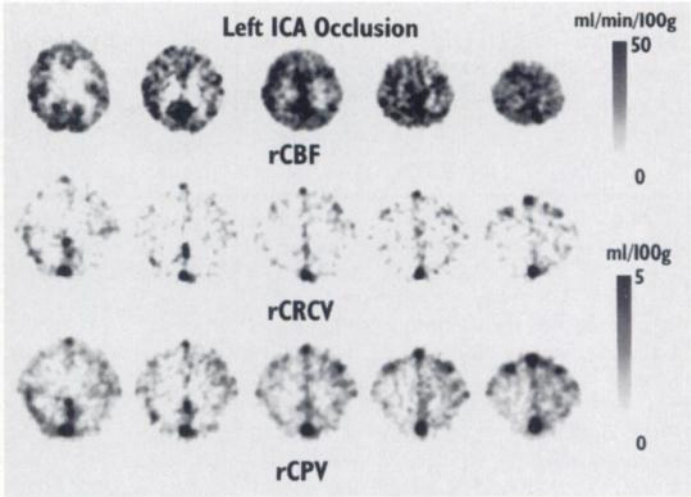

FIGURE 4. Images showing CBF, rCRCV and rCPV in a patient with left ICA occlusion. Note the greater increase in rCPV than rCRCV in the hypoperfused area.

and regional Hct obtained from 24 ROIs on the cerebral hemispheres of the 12 normal volunteers. The average regional cerebral Hct was 38.3 ± 3.45% and the mean cerebral/large-vessel Hct ratio was 0.88 ± 0.06. No significant difference was found between the right and left hemispheres. The result obtained with the method of Lammertsma et al. (*11*) was 0.88 ± 0.07 for the cerebral/large-vessel Hct ratio, and no significant difference was observed compared with our method. In the sinuses, the mean Hct ratio was 1.03 ± 0.05.

Table 3 shows the normal values of the rCRCV, rCPV, regional cerebral Hct and Hct ratio in the gray matter, white matter and basal ganglia obtained from six healthy volunteers. Although the average rCRCV and rCPV values were greater in the gray matter than in the white matter, the regional Hct and Hct ratios were similar in both areas. No significant differences between the right and left were seen in any area. Figure 3 displays the average rCRCV, rCPV and Hct ratio for each area and the differences among those areas. The rCRCV and rCPV values were significantly smaller in the white matter than in the cortex or basal ganglia. No significant differences were found between the gray matter and the basal ganglia. However, the Hct ratio in the basal ganglia was significantly greater than in the gray or white matter.

Patients

Table 4 summarizes the mean values of each variable in hypoperfused and normal hemispheres in the seven patients. Increases in the CBV, OEF, rCRCV and rCPV and decreases in the $CMRO_2$ and cerebral Hct were seen in the hypoperfused hemispheres. Significant differences were seen in the CBF, OEF, rCPV, cerebral Hct and Hct ratio ($p < 0.05$, paired *t*-test). Figure 4 demonstrates a greater increase in rCPV than rCRCV in the hypoperfused area of a patient with occlusion of the left internal carotid artery (ICA).

DISCUSSION

Feasibility of Plasma-Pool Imaging

The major purpose of the present study was to evaluate the clinical feasibility of ^{62}Cu-HSA-DTS for PET imaging. Copper-62-HSA-DTS is considered an important tracer for plasma-pool imaging not only in PET centers without an in-house cyclotron, but also in those with a cyclotron for measuring regional cerebral Hct. Copper-62-HSA-DTS can be easily labeled, and its image quality was excellent compared with the CBV image obtained by the $C^{15}O$ bolus inhalation method because of its longer physical half-life (9.74 min) and longer scanning time. In fact, the S/N ratio of the ^{62}Cu-HSA-DTS images was greater than that of the $C^{15}O$ images. The scan in the ^{62}Cu-HSA-DTS study started at 3 min after the injection and lasted for 8 min because the half-life was approximately 10 min, and a longer scan time than that used in the present study was not considered to provide better image quality. A previous in vivo study in rabbits found that the blood clearance of ^{62}Cu-HSA-DTS was similar to that for ^{131}I-HSA, a well-established radiopharmaceutical for plasma volume studies, and the radioactivity in the blood was almost stable from 5 to 15 min (*7*). Although the stability of ^{62}Cu-HSA-DTS in the plasma was not measured in the present study, more than 97% of the blood activity was counted in the plasma for 11 min after the injection, indicating excellent characteristics for plasma-pool imaging. Combination of ^{62}Cu-HSA-DTS and $C^{15}O$ makes it possible to easily measure the rCPV, rCRCV and regional cerebral Hct by PET.

Regional Cerebral Hematocrit

The second purpose of the present study was to measure the regional cerebral Hct in normal subjects and in patients with

TABLE 2
Regional Cerebral Red Cell Volume, Regional Plasma Volume and Hematocrit in 12 Healthy Volunteers*

Measure	Right hemisphere	Left hemisphere	Mean
rCRCV (ml/100 g)	0.98 ± 0.16	0.97 ± 0.11	0.98 ± 0.14
rCPV (ml/100 g)	1.59 ± 0.26	1.57 ± 0.22	1.58 ± 0.24
Cerebral Hct (%)	38.2 ± 3.71	38.3 ± 3.38	38.3 ± 3.45
Hct ratio	0.87 ± 0.06	0.88 ± 0.05	0.88 ± 0.06

*Data are mean value ± s.d. at slice level 70 mm above the orbitomeatal line.
rCRCV = regional cerebral red cell volume; rCPV = regional cerebral plasma volume; Hct = hematocrit.

TABLE 3
Regional Cerebral Red Cell Volume, Regional Cerebral Plasma Volume and Regional Cerebral Hematocrit Ratio in Six Healthy Volunteers*

Region	rCRCV (ml/100 g)	rCPV (ml/100 g)	Regional Hct (%)	Hct ratio
Right gray matter	1.30 ± 0.27	2.21 ± 0.42	37.0 ± 4.5	0.85 ± 0.08
Left gray matter	1.33 ± 0.27	2.26 ± 0.47	37.1 ± 3.7	0.85 ± 0.06
Mean	1.31 ± 0.26	2.23 ± 0.43	37.0 ± 3.9	0.85 ± 0.07
Right white matter	0.74 ± 0.12	1.23 ± 0.26	37.6 ± 3.1	0.87 ± 0.07
Left white matter	0.71 ± 0.12	1.22 ± 0.19	36.7 ± 4.0	0.84 ± 0.07
Mean	0.72 ± 0.12	1.23 ± 0.22	37.2 ± 3.4	0.86 ± 0.07
Right basal ganglia	1.35 ± 0.28	2.04 ± 0.28	39.9 ± 2.4	0.92 ± 0.04
Left basal ganglia	1.36 ± 0.33	1.99 ± 0.33	40.4 ± 2.5	0.93 ± 0.04
Mean	1.35 ± 0.22	2.02 ± 0.31	40.2 ± 2.4	0.92 ± 0.04

*Data are mean value ± s.d.; slice levels were 70 mm above the orbitomeatal line in gray and white matter and 40 mm above in basal ganglia.
rCRCV = regional cerebral red cell volume; rCPV = regional cerebral plasma volume; Hct = hematocrit.

cerebrovascular disease. Previous studies have reported cerebral Hct to be smaller than that of large vessels (*9–15*), and a regional cerebral/large-vessel Hct ratio *(r)* of 0.85 has generally been accepted for correction of the cerebral Hct in measurement of the rCBV by PET with $C^{15}O$ as a marker of the red cell volume (*21,22*). Recently, several investigators reported the Hct ratio to be smaller than 0.85 when measured by PET or SPECT (*11–13*). Although Lammertsma et al. (*11*) reported that the mean Hct ratio in nine subjects was 0.69 ± 0.07, except for one normal subject, the subjects were all patients with a brain tumor or cerebrovascular disease. The greatest number of normal subjects was studied by Sakai et al. (*12*) using SPECT, and they reported an Hct ratio of 75.9 ± 2.1% for 10 healthy subjects, which was approximately 10% lower than 85%. In the present study, the mean Hct ratio was 0.88 ± 0.06 for the 24 normal cerebral hemispheres of the 12 normal subjects, which was greater than 0.85, and *r* was 1.03 ± 0.05 in the sinuses. If the Hct in the sinuses is considered to be the same as that in the major vessels, the cerebral Hct ratio is corrected to 0.85. The cerebral activity and cerebral/blood ratio may change within the first 10 min (*11*); thus, the earlier scan timing in the present study may have caused the difference in the Hct ratio. However, the Hct ratio of almost 1.0 in the sinuses seems to validate the accuracy of our methods. Loutfi et al. (*14*) reported the cerebral Hct ratio in three normal subjects (six hemispheres) to be 0.81–0.90 (mean 0.87 ± 0.03) and 0.94–1.00 in the sinuses, consistent with our findings. In addition, they reported that the mean Hct ratio in 15 patients with cerebrovascular disease was 0.77 ± 0.07 in 30 cerebral hemispheres and 0.85 ± 0.06 in the sinuses. By performing correction using *r* in the sinuses, the Hct ratio of patients in their study was 0.90. The correction for the Hct in the sinuses is considered to be a reasonable method for measurement of the cerebral Hct. The calculations with the method of Lammertsma et al. (*11*) using the data of present study revealed results similar to those calculated by our method. Although our method requires measurement of plasma count, both rCRCV and rCPV can be measured directly, and calculation of the regional cerebral Hct is simple.

No differences were observed in the rHct or Hct ratio in the gray matter and white matter at the level of the centrum semiovale in the six healthy subjects. This result is consistent with the report of Lammertsma et al. (*11*). In the basal ganglia, however, the regional Hct and Hct ratio were larger than that in the gray and white matter. In this area, the blood pool in large vessels might affect the brain tissue count. However, the main reason for this result was the lower rCPV in the basal ganglia than in the other cortices despite the similar value for the rCRCV (Table 3). If the radioactivity in the large vessels affects the tissue count, the values of rCPV should also be affected. A significant difference was found between the gray matter and the basal ganglia when the values of rCPV were compared by the paired t-test, whereas no difference was seen in the values of rCRCV. With our method, the CBV image can be calculated directly by simple addition of the rCRCV and rCPV images without correction for the inhomogeneity of the regional Hct ratio in the brain.

Regional Hematocrit in Cerebrovascular Disease

In the patients with cerebrovascular disease, significant decreases in the regional cerebral Hct and Hct ratio were observed in the hypoperfused side compared with the normal side. Although the Hct ratio in the normal hemisphere was slightly higher than the mean value in the normal subjects, the Hct ratios of the patients were calculated using the Hct of arterial blood samples. The average Hct values of the peripheral arterial blood and venous blood in the seven patients were 35.8 ± 1.63% and 37.3 ± 1.73%, respectively. If the Hct ratio of the patients is corrected with the mean values of the arterial and venous Hct, the Hct ratio on the normal side is 0.86. Further, the Hct ratio on the occluded side is corrected to be 0.82, which is significantly lower than the normal side. The decrease in the regional Hct on the occluded side was caused by the significant increase in rCPV and almost stable rCRCV (Table 4). Because all seven patients were in the chronic phase of major vascular occlusion at least 1 mo after onset, it is not likely that there was leakage of ^{62}Cu-HSA-DTS across the blood-brain barrier (BBB) into the brain parenchyma, causing an increase in the regional retention of the tracer. In fact, all patients but one had no major infarction, and the affected hemispheres were not enhanced on the CT or MRI study in any of the patients. Compensation for oxygen metabolism seemed to have occurred because no significant decrease in $CMRO_2$ was observed on the occluded side. In the report of Loutfi et al. (*14*), a significantly higher regional Hct value was observed on the affected side in three of eight patients with stroke. However, their study was performed in the acute phase of ischemic attack, which was different from our study, and four of eight patients

TABLE 4
Regional Cerebral Blood Flow, Cerebral Blood Volume, Oxygen Metabolism and Hematocrit in Seven Patients with Cerebrovascular Disease (mean ± s.d.)

Measure	Occlusion side	p value*	Normal side
CBF (ml/min/100 g)	25.6 ± 6.77	<0.05	30.3 ± 6.57
CBV (ml/100 g)	2.93 ± 0.76	ns	2.80 ± 0.49
$CMRO_2$ (ml/min/100 g)	1.82 ± 0.29	ns	2.04 ± 0.32
OEF	0.45 ± 0.06	>0.05	0.42 ± 0.05
rCRCV (ml/100 g)	0.87 ± 0.12	ns	0.86 ± 0.18
rCPV (ml/100 g)	2.01 ± 0.33	>0.05	1.81 ± 0.26
Cerebral Hct (%)	30.4 ± 4.23	<0.05	32.2 ± 5.25
Hct ratio	0.85 ± 0.05	<0.05	0.90 ± 0.08

*Paired t-test, occlusion side versus normal side.
CBF = cerebral blood flow; CBV = cerebral blood volume; ns = not significant; $CMRO_2$ = cerebral metabolic rate of oxygen; OEF = oxygen extraction fraction; rCRCV = regional cerebral red cell volume; rCPV = regional cerebral plasma volume; Hct = hematocrit.

with stroke and six of six patients with a transient ischemic attack showed no significant difference between both hemispheres. One patient in their study underwent SPECT twice, in the acute and subacute phases (1 and 6 days, respectively, after the onset of stroke). The affected hemisphere showed a significantly higher regional cerebral Hct than the uninvolved hemisphere in the acute phase, but in the subacute phase it decreased to a value similar to that in the uninvolved hemisphere. Another patient with multi-infarct dementia in the study of Lammertsma et al. (*11*) showed a lower Hct ratio than the other patients (r = 0.59). In the chronic phase, sufficient compensation for cerebral ischemia might cause an increase in rCPV, which may decrease blood viscosity and improve the microcirculation. Further study of cerebrovascular disease is needed to elucidate the details of the cerebral microcirculation.

Possible Limitations

There are some limitations on the use of ^{62}Cu-HSA-DTS for measuring plasma volume and regional cerebral Hct. One is the possibility of leakage of this compound into the cerebral parenchyma in the case of acute injury or a brain neoplasm, where the BBB may not be intact. In the case of such leakage, rCPV may increase and Hct may decrease in the affected areas compared with the areas where the BBB is intact. Another limitation is that the short half-life of ^{62}Cu (10 min) does not permit a longer scanning time. Because the method assumes an equilibrium state in the vascular space after administration of the tracer, the scanning time in the present study might be too early, especially in diseased areas such as a vascular-rich tumor. To clarify the scope of these limitations, further investigation is needed using ^{11}CO and dynamic PET imaging.

CONCLUSION

The results in both normal subjects and patients with cerebrovascular disease demonstrated the possibility of heterogeneity in regional cerebral Hct and the Hct ratio (r), even in the global comparison of hemispheres. These findings suggest that measurement of the regional Hct may provide useful information for assessment of the cerebral circulation. Copper-62-HSA-DTS appears to be useful for measurement of the plasma volume and regional Hct in clinical studies.

ACKNOWLEDGMENTS

We thank Y. Ouchi, MD, and Y. Nagahama, MD, for their invaluable clinical assistance and suggestions, and Mr. H. Kitano and Mr. H. Taniuchi for their excellent technical assistance.

REFERENCES

1. Robinson GD, Zielinski FW, Lee AW. The zinc-62/copper-62 generator: a convenient source of copper-62 radiopharmaceuticals. *Int J Appl Radiat Isot* 1980;31:111–116.
2. Green MA. A positron copper radiopharmaceutical for imaging the heart and brain: copper-labeled pyruvaldehyde bis(N_4-methylthiosemicarbazone). *Nucl Med Biol* 1987; 14:59–61.
3. Green MA, Klippenstein DL, Tennison JR. Copper(II) bis(thiosemicarbazone) complexes as potential tracers for evaluation of cerebral and myocardial blood flow with PET. *J Nucl Med* 1988;29:1549–1557.
4. Mathias CJ, Welch MJ, Raichle ME, et al. Evaluation of a potential generator-produced PET tracer for cerebral perfusion imaging: single-pass cerebral extraction measurements and imaging with radiolabeled Cu-PTSM. *J Nucl Med* 1990;31:351–359.
5. Green MA, Mathias CJ, Welch MJ, et al. Copper-62-labeled pyruvaldehyde bis(N4-methylthiosemicarbazonato)copper(II): synthesis and evaluation as a positron emission tomography tracer for cerebral and myocardial perfusion. *J Nucl Med* 1990;31:1989–1996.
6. Okazawa H, Yonekura Y, Fujibayashi Y, et al. Clinical application and quantitative evaluation of generator-produced ^{62}Cu-PTSM as a brain perfusion tracer for PET. *J Nucl Med* 1994;35:1910–1915.
7. Fujibayashi Y, Matsumoto K, Arano Y, Yonekura Y, Konishi J, Yokoyama A. ^{62}Cu-labeling of human serum albumin-dithiosemicarbazone (HSA-DTS) conjugate for regional plasma volume measurement: application of new ^{62}Zn/^{62}Cu generator system. *Chem Pharm Bull (Tokyo)* 1990;38:1946–1948.
8. Mathias CJ, Welch MJ, Green MA, et al. In vivo comparison of copper blood-pool agents: potential radiopharmaceuticals for use with copper-62. *J Nucl Med* 1991;32: 475–480.
9. Larsen OA, Lassen NA. Cerebral hematocrit in normal man. *J Appl Physiol* 1964;19:571–574.
10. Oldendorf WH, Kitano M, Shimizu S, Oldendorf SZ. Hematocrit of the human cranial blood pool. *Circ Res* 1965;17:532–539.
11. Lammertsma AA, Brooks DJ, Beaney RP, et al. In vivo measurement of regional cerebral hematocrit using positron emission tomography. *J Cereb Blood Flow Metab* 1984;4:317–322.
12. Sakai F, Nakazawa K, Tazaki Y, et al. Regional cerebral blood volume and hematocrit measured in normal human volunteers by single-photon emission computed tomography. *J Cereb Blood Flow Metab* 1985;5:207–213.
13. Brooks DJ, Beaney RP, Lammertsma AA, et al. Studies on regional cerebral hematocrit and blood flow in patients with cerebral tumors using positron emission tomography. *Microvasc Res* 1986;31:267–276.
14. Loutfi I, Frackowiak RSJ, Myers MJ, Lavender JP. Regional brain hematocrit in stroke by single-photon emission computed tomography imaging. *Am J Physiol Imaging* 1987;2:10–16.
15. Frackowiak RSJ. Measurement of local hematocrit, energy metabolism and hemodynamics in cerebral ischemia with positron tomography. *Acta Neurol Scand* 1989;127 (suppl):14–21.
16. Fujibayashi Y, Matsumoto K, Yonekura Y, Konishi J, Yokoyama A. A new zinc-62/copper-62 generator as a copper-62 source for PET radiopharmaceuticals. *J Nucl Med* 1989;30:1838–1842.
17. Sadato N, Yonekura Y, Senda M, et al. PET and the autoradiographic method with continuous inhalation of oxygen-15-gas: theoretical analysis and comparison with conventional steady-state methods. *J Nucl Med* 1993;34:1672–1680.
18. Frackowiak RSJ, Lenzi GL, Jones T, Heather JD. Quantitative measurement of regional cerebral blood flow and oxygen metabolism in man using ^{15}O and positron emission tomography: theory, procedure and normal values. *J Comput Assist Tomogr* 1980;4:727–736.
19. Lammertsma AA, Jones T. Correction for the presence of intravascular oxygen-15 in the steady-state technique for measuring regional oxygen extraction ratio in the brain: 1. Description of the method. *J Cereb Blood Flow Metab* 1983;3:416–424.
20. Sadato N, Yonekura Y, Senda M, et al. Noninvasive measurement of regional cerebral blood flow change with $H_2{}^{15}O$ and positron emission tomography using a mechanical injector and a standard arterial input function. *IEEE Trans Med Imag* 1993;MI-12: 703–710.
21. Phelps ME, Grubb RL, Ter-Pogossian MM. Correlation between PaCO2 and regional cerebral blood volume by x-ray fluorescence. *J Appl Physiol* 1973;35:274–280.
22. Phelps ME, Huang SC, Hoffman EJ, Kuhl DE. Validation of tomographic measurement of cerebral blood volume with ^{11}C-labeled carboxyhemoglobin. *J Nucl* 1979;20: 328–334.